Research Article

Journal of PeptideScience

Received: 24 May 2011 Revised: 6 October 2011 Accepted: 17 October 2011 Published online in Wiley Online Library: 2 March 2012

(wileyonlinelibrary.com) DOI 10.1002/psc.1431

Interaction of L-leucyl-L-leucyl-L-leucine thin film with water and organic vapors: receptor properties and related morphology

Marat A. Ziganshin,[a]* Irina G. Efimova,[a] Valery V. Gorbatchuk,[a] Sufia A. Ziganshina,[b] Anton P. Chuklanov,[b] Anastas A. Bukharaev[b] and Dmitry V. Soldatov[c]

The ability of highly ordered tripeptide structures to keep or change their morphology in contact with organic vapors was studied. A thin film of tripeptide L-leucyl-L-leucyl-L-leucine (LLL) was prepared having microcrystals and nanocrystals on its surface, which are stable upon vacuum drying but become objects of selective morphology change after a contact with vapors of organic solvents. Fine separate LLL crystals and their agglomerates of submicron and larger dimensions were observed by atomic force microscopy and scanning electron microscopy. After saturation with guest vapors, these crystals can remain intact or change their morphology with the increase in size or complete destruction depending on the guest molecular structure. The crystals completely lose their shape after the binding of pyridine vapors. The other studied guests produce much smaller transformations or have no effect on crystal morphology despite being sorbed by solid LLL, which was shown using quartz crystal microbalance sensor. The observed size-exclusion effect for guest sorption by LLL was found to be broken by the same guests that can change the initial crystal shape. This helps to explain the morphology changes of LLL crystals after the guest sorption and release.

Supporting information may be found in the online version of this article.

Keywords: tripeptide; quartz crystal microbalance; atomic force microscopy; scanning electron microscopy; supramolecular receptors; surface morphology; sorption

Introduction

Peptides forming highly ordered structures are interesting materials for recognition, binding and storage of gaseous compounds [1–3]; encapsulation of neutral organic solvents [4,5]; creating membranes [6], superhydrophobic surfaces [7] and ionic channels [8,9]; and separation of enantiomers [10–12]. For this, various structures with hydrophilic or hydrophobic nanochannels [2,4,13], layered crystals with two-dimensional or three-dimensional network of hydrogen bonds [2,5], can be prepared by crystallization of peptides from liquid solutions. Such materials can be used in bionanotechnology [6,14–16] and nanomedicine [6,17–20] because of their non-toxicity, biocompatibility and ecological acceptability [21–24].

Generally, peptide frameworks remain stable after the solvent removal [4,25], which is important for their applications. A specific H-bonded self-assembly of peptides, which supports their structural stability, may define also their selectivity with size restrictions on the binding of neutral guests. For example, a strong 'size exclusion effect' was observed for similar objects – dry proteins [26,27]. One can expect such size exclusion effect from peptide structures as far as their H-bonded framework remains intact.

Similar to hydrated proteins [28], the peptides are considered as 'soft materials' [29], which can change their packing under external stimuli, e.g. in interaction with some substrate (guest) [2]. For example, the interaction of amorphous diphenylalanine film with water or organic vapor may give highly ordered nanowires or nanotubes [30–32]. The morphology change of L-alanyl-L-valine film after binding of organic vapors was visualized by atomic force microscopy (AFM) [33]. This 'softness' may complicate the relationship between a guest-binding capacity of peptide and the guest size. A guest, which breaks the peptide H-bonded structure, may break also a size-exclusion effect. Such loss of size-exclusion effect was observed, e.g. for initially dry

* *Correspondence to: Butlerov Institute of Chemistry, Kazan (Volga Region) Federal University, Kremlevskaya ul. 18, Kazan, 420008 Russia. E-mail: Marat.Ziganshin@ksu.ru*

a *Butlerov Institute of Chemistry, Kazan (Volga Region) Federal University, Kremlevskaya ul. 18, Kazan 420008, Russia*

b *Zavoisky Physical-Technical Institute, Kazan Scientific Center, Russian Academy of Sciences, Sibirskii trakt 10/7, Kazan 420029, Russia*

c *University of Guelph, 50 Stone Road East, Guelph, Ontario, Canada, N1G 2W1*

protein upon hydration [34]. Therefore, the structure–property relationships for guest binding by peptides and for stability of their highly ordered structures in contact with guest may be similar.

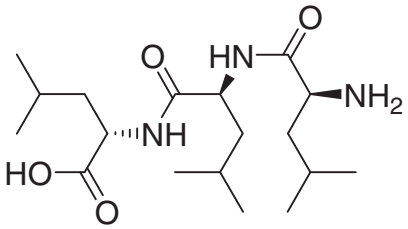

LLL

In present work, these structure–property relationships were studied for tripeptide L-leucyl-L-leucyl-L-leucine (LLL). This tripeptide forms well-defined monoclinic or triclinic crystals with β-sheet structures when crystallized from methanol [5]; pyridine; or α-picoline, β-picoline and γ-picoline [24] solutions. An ability of various guests to destroy such LLL crystals was studied using AFM. Besides, the binding capacity of LLL film for vapors of water and several organic guests was determined using quartz crystal microbalance (QCM). The correlation between the guest-binding capacity and induced morphology changes of LLL film depending on the guest size and H-bonding ability was analyzed.

Materials and Methods

Materials

Tripeptide LLL (Chem-Impex) was used without additional purification. The purity of the studied organic guests dried using standard techniques [35] was tested using gas chromatography to be better than 99.5%.

QCM Study of Guest Binding

In the present study, a sensor device with 10 MHz QCM crystals (Part No. 151620–10; ICM Co. Inc., USA) of thickness shear mode was used [36]. The tripeptide coatings (~0.65 μg) were prepared by dropping and drying (for 2 min) using hot air (45 °C) of methanol solution on the gold surface of quartz crystals. These coatings with an average thickness of 40 nm give a decrease of $F \sim 800$ Hz in the crystal frequency after solvent removal. The thickness value was estimated by the layer area, mass and density of crystal LLL with methanol $\rho = 1.051$ g/cm^3, calculated from X-ray single crystal data [5].

In a typical QCM sensor experiment, a liquid guest was sampled using microsyringe to the sensor cell bottom through a dosing hole in the cell cover. The sampled guest amount was twice as large as necessary to create a saturation vapor in the sealed cell. Still, the cell was made not to be hermetic during sensor experiment to avoid guest condensation on the crystal coating surface. The guest relative vapor pressure P/P_0 was kept below saturation level by the vapor leak through the dosing hole. This level is equal to $P/P_0 = 0.85$ [37]. A sensor baseline noise did not exceed 2 Hz. The frequency change of quartz crystal ΔF in sensor experiments was determined with the reproducibility of 5% for $\Delta F > 50$ Hz.

To regenerate the tripeptide coatings after the guest binding, they were dried using hot air as described earlier. This regeneration procedure was repeated at least twice until the constant sensor frequency was achieved. Such procedure gave the value of frequency change corresponding to initial coating prepared from the methanol solution. The residual water content (3% w/w) in this coating was determined using the frequency increase of coated quartz crystals equilibrated over P_4O_{10} powder for 2000 s. The same value was obtained with a piece of sodium metal as the drying agent.

Atomic Force Microscopy

The AFM images in topography and phase modes were recorded using the atomic force microscope Solver P47 (NT-MDT, Russia). Measurements were performed in air using a tapping mode. Standard silicon cantilevers NSG-11 (NT-MDT) were used. Scan speed was in the range of 0.5–0.9 line/s.

For AFM experiments, tripeptide films with diameter of 3 mm were prepared on the surfaces of highly oriented pyrolytic graphite (HOPG) plates (1 × 1 cm) using the same technique as for QCM study. HOPG was freshly cleaved before use. In these experiments, first, an AFM image was obtained for the initial tripeptide film dried off methanol solvent. Then the tripeptide layer was saturated with organic or water vapors. Thereafter, the guest was removed from the film as described earlier for sensor experiment, and an AFM image of the same film region was obtained.

Scanning electron microscopy

For scanning electron microscopy (SEM), a sample of tripeptide film was prepared on the surfaces of HOPG as for AFM studies. Then it was dried in vacuum (10 Pa) during 12 h before the experiment. SEM images were recorded using a scanning electron microscope Evo 50 (Carl Zeiss, Germany) at 20 kV.

Results and Discussion

QCM Study of Guest Binding

The QCM sensor responses ΔF of quartz crystals coated with LLL were determined for vapors of 11 organic guests and water with relative vapor pressure of $P/P_0 = 0.85$ at 298 K. Typical sensor responses for guest vapors are given on Figure 1 and ESI.

The equilibration time in this experiment was in the range from 130 s for nitromethane (Figure 1B) to more than 1600 s for pyridine vapor sorption (ESI).

The guest/host molar ratio S (Table 1) was calculated using the equation

$$S = (\Delta F/\Delta F_{LLL})(M_{LLL}M_{guest})$$

where ΔF_{LLL} is a frequency change corresponding to the tripeptide mass, corrected on the residual water content in the air-dried coating (3% w/w). M_{LLL} and M_{guest} are molar weights of tripeptide and guest, respectively. The observed values of guest content S in LLL saturated with methanol and pyridine are in good agreement with single crystal XRD data for corresponding inclusion compounds (Table 1).

A general picture of tripeptide selectivity for guest vapors may be seen in the correlation between stoichiometry of the complexes S and guest molar refraction MR_D (Figure 2). Molar refraction is a good parameter of molecular size [38,39]. There is a general decrease of guest content S with the increase of guest size, which indicates a size exclusion effect for guest molecules. The sorption capacity of LLL for vapors of aliphatic alcohols decreases approximately on 20% for each added methylene group.

Journal of PeptideScience

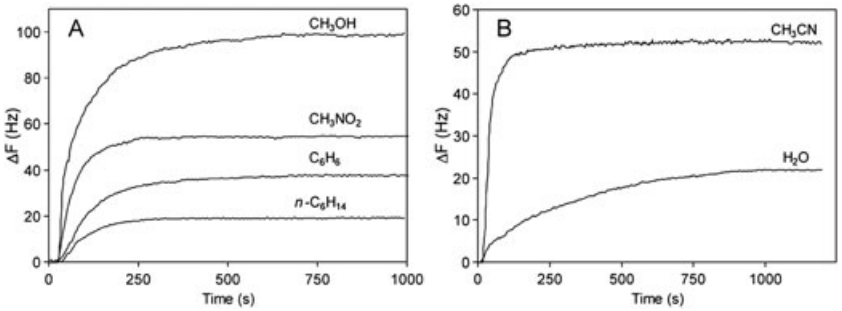

Figure 1. Responses of QCM sensor coated with LLL to organic vapors with the relative vapor pressure of $P/P_0 = 0.85$ at $T = 298$ K. Sensor responses ΔF are normalized to the coating mass with corresponding frequency decrease of $\Delta F_{LLL} = 800$ Hz.

A difference in guest H-bonding properties may explain the observed dependence of LLL guest-sorption capacity *S* on the group composition of guest molecules. Guest pairs with nearly the same molecular size but with different H-bonding ability, such as ethanol and nitromethane, pyridine and benzene, have *S* values differing by three and four times, respectively (Table 1 and Figure 2). The highest sorption capacity *S* of LLL for alcohols and pyridine may be because of the ability of these guests to form H-bonds with tripeptide, as it was found for methanol [5] and pyridine [24].

Besides, LLL is more selective for *n*-propanol than for isopropanol, which is similar to the binding selectivity of albumin [34], trypsin [40], cross-linked poly(*N*-6-aminohexylacrylamide) [41] and phosphorus-containing dendrimer of fourth generation [42] for these isomers. The observed lower sorption capacity of LLL for water than for alcohols indicates a rather hydrophobic nature of this tripeptide.

Table 1. The guest/host molar ratio calculated from QCM sensor data

Guest	MR_D[a] (cm^3/mol)	*S* (mol guest/mol LLL)
H_2O	3.7	0.56 ± 0.03
CH_3OH	8.2	1.41 ± 0.08; 1.5[b]
CH_3CN	11.1	0.59 ± 0.03
CH_3NO_2	12.5	0.42 ± 0.02
C_2H_5OH	13.0	1.22 ± 0.06
n-C_3H_7OH	17.5	0.94 ± 0.05
i-C_3H_7OH	17.6	0.87 ± 0.04
n-C_4H_9OH	22.1	0.78 ± 0.03
C_5H_5N	24.2	0.87 ± 0.03; 1.0[c]
C_6H_6	26.3	0.22 ± 0.02
n-C_6H_{14}	29.9	0.10 ± 0.01
$C_6H_5CH_3$	31.1	0.18 ± 0.01

[a] $MR_D = (M/d) \times (n_D^2 - 1)/(n_D^2 + 2)$, where *M* is molecular weight of organic compound, *d* and n_D are density and refractive index of liquid guest, respectively.
[b] X-ray data from Ref. [5].
[c] X-ray data from Ref. [24].

Morphology of Tripeptide Thin Layer

To get detailed information on the guest effect on the morphology of LLL film prepared from methanol solution, its surface was studied in dried state on HOPG using AFM and SEM.

According to the SEM image (Figure 3) the initial LLL film is covered with microcrystals and nanocrystals. The most LLL crystals have the shape of parallelograms or their combinations with the edge length from 250 nm to 5 μm (Figure 3). The crystals with different top faces were observed. More of them have angles of $87 \pm 3°$ and $94 \pm 2°$. This fits to the X-ray diffraction data for LLL clathrate with methanol and water, which unit cell angles are $\alpha = 90°$, $\beta = 97.29°$ and $\gamma = 90°$ [23]. Less crystal faces have angles of $74 \pm 3°$ and $105 \pm 3°$. The SEM image of the film from the same experiment in a smaller scale and image of pure HOPG are given in ESI.

The surface of separate tripeptide microcrystal was characterized by AFM in topography mode (Figure 4A and ESI) and in phase contrast mode (Figure 4B). The phase contrast image proves that the LLL crystal lies on the more amorphous film of tripeptide, not directly on the surface of HOPG. Both images on Figure 4 show

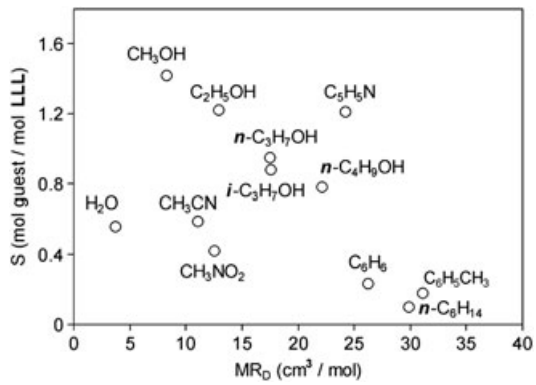

Figure 2. Correlation of the guest/host molar ratio *S* in inclusion compounds of LLL with guest molar refraction MR_D.

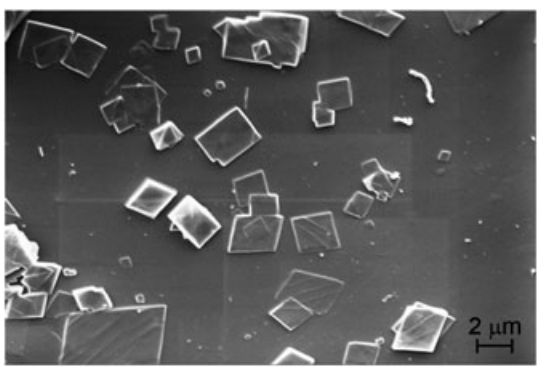

Figure 3. SEM image of initial LLL film deposited on HOPG from methanol solution and dried using hot air (45 °C) for 2 min.

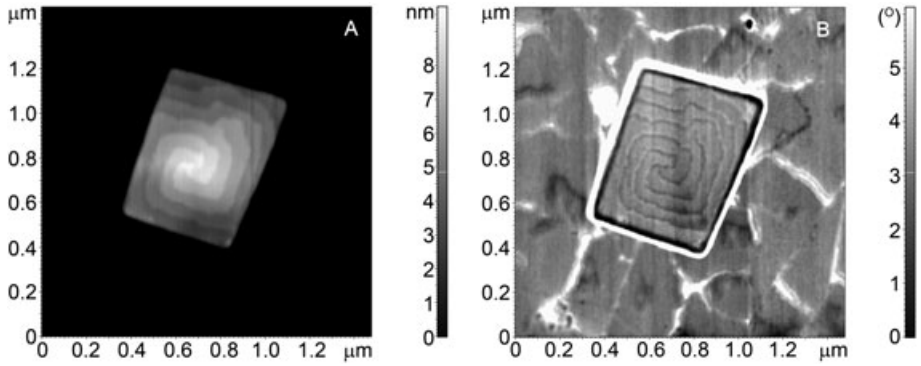

Figure 4. AFM images of LLL crystal on the surface of initial dried film deposited on HOPG from a methanol solution: obtained in topography mode (A) and in phase contrast mode (B). Before AFM experiment, LLL film was dried using hot air (45 °C) for 2 min.

the growth terraces on the crystal face. So, its surface has an ordinary rectangular pyramidal structure. The average width and height of its growth steps are 55 and 1.3 nm, respectively. The last value is in agreement with the cell lengths $a = 12.031$, $b = 15.578$ and $c = 14.087$ Å of LLL clathrate hydrate with methanol [23]. The height of this crystal in its center is equal to 9 nm (Figure 4A).

For LLL film deposited on HOPG from methanol solution, the effect of saturation with guest vapors on surface morphology

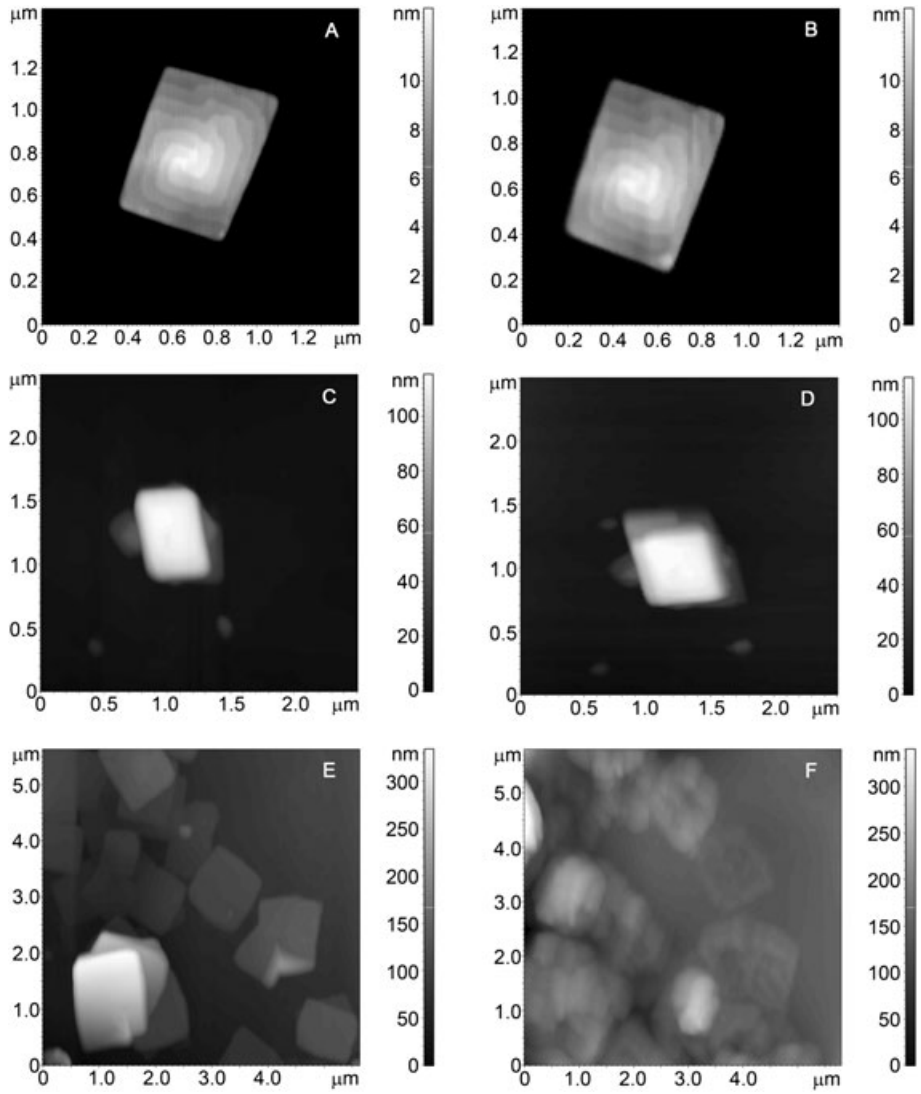

Figure 5. AFM images of the surface of the initial film with crystals of LLL deposited on HOPG from a methanol solution (A), (C) and (E) and the film and crystals of LLL saturated with water vapors for 92 min (B), nitromethane vapors for 17 min (D) and pyridine vapors for 110 min (F). Before AFM experiment, LLL films were dried using hot air (45 °C) for 2 min.

Journal of PeptideScience

was studied using AFM. For each guest, the saturation time was enough to reach the saturation of LLL film in QCM sensor experiment (Figure 1).

The LLL crystal, as shown in Figures 5A and 5B, remains undamaged after saturation with water vapor. The angles of its top face parallelogram become a little different, but this difference is within experimental errors. The terrace structure also did not change. No change of crystal morphology was observed also after LLL saturation with *n*-hexane vapor (ESI).

Small changes in morphology of LLL crystals were found after saturation of the initial film with nitromethane vapor (Figures 5C and 5D) and with vapors of methanol and toluene (ESI). In these cases, an insignificant stratification of crystalline agglomerates, displacement of the crystals relative to each other and slight variations in their lateral dimensions were observed. The height of the crystals remains practically unchanged. The saturation of LLL film with pyridine vapor gives a significant change of microcrystals. They become loose and shapeless (Figures 5E and 5F).

The observed different ability of the studied guests to change morphology of LLL crystals correlates with the structure–property relationship between LLL sorption capacity S and guest molar refraction MR_D (Table 1 and Figure 2). Because of a free volume in LLL crystal structure is restricted according to X-ray data [20,23], one can expect larger changes of LLL crystal for guests with higher S and MR_D values. According to Table 1, the product $S \times MR_D$ changes for the studied guests in the order $H_2O < C_6H_{14}$ $CH_3NO_2 < C_6H_5CH_3 < CH_3OH < C_5H_5N$. This coincides with the order of the observed ability of these guests for destruction of LLL crystals. So, the data on vapor binding capacity of the studied tripeptide can be used for prediction of its molecular packing stability in contact with organic vapors.

Conclusions

An essential dependence of the guest-induced changes in the nanocrystal morphology of LLL tripeptide on the guest molecular structure was found. An ability of guest to destroy LLL single crystals depends both on the guest size and H-bonding capacity. The pattern of this dependence correlates with the structure–property relationship observed for QCM sensor responses of LLL thin film for nearly saturated guest vapors under comparable conditions. This correlation makes much easier the search of solvents and guests that may keep, modify or destroy highly ordered peptide structure. Instead of expensive SEM and AFM microscopy studies, very simple QCM sensor experiment may be used in a preliminary screening of solvents and substrates for potential peptide applications.

Acknowledgements

This work was supported by grant RFBR No. 09-03-97011-volga region and Federal Program 'Research and scientific-pedagogical personnel of Innovative Russia' for 2009–2013 (Gov. Contract No. P2345). Authors thank Dr Y. N. Osin, Zavoisky Physical-Technical Institute, Kazan, Russia, for SEM experiments.

References

1 Comotti A, Bracco S, Distefano G, Sozzani P. Methane, carbon dioxide and hydrogen storage in nanoporous dipeptide-based materials. *Chem. Commun.* 2009; 284–286.
2 Görbitz CH. Microporous organic materials from hydrophobic dipeptides. *Chem. Eur. J.* 2007; **13**: 1022–1031.
3 Wright PA. Opening the door to peptide-based porous solids. *Science* 2010; **329**: 1025–1026.
4 Görbitz CH. An exceptionally stable peptide nanotube system with flexible pores. *Acta Crystallogr. B* 2002; **58**: 849–854.
5 Go K, Parthasarathy R. Crystal structure and a twisted β-sheet conformation of the tripeptide L-leucyl-L-leucyl-L-leucine monohydrate trimethanol solvate: conformation analysis of tripeptides. *Biopolymers* 1995; **36**: 607–614.
6 Zhao X, Pan F, Xu H, Yassen M, Shan H, Hauser CAE, Zhang S, Lu JR. Molecular self-assembly and applications of designer peptide amphiphiles. *Chem. Soc. Rev.* 2010; **39**: 3480–3498.
7 Lee JS, Ryu J, Park CB. Bio-inspired fabrication of superhydrophobic surfaces through peptide self-assembly. *Soft Matter.* 2009; **5**: 2717–2720.
8 Percec V, Dulcey AE, Balagurusamy VSK, Miura Y, Smidrka J, Peterca M, Nummelin S, Edlund U, Hudson SD, Heiney PA, Duan H, Magonov SN, Vinogradov SA. Self-assembly of amphiphilic dendritic dipeptides into helical pores. *Nature* 2004; **430**: 764–768.
9 Fernandez-Lopez S, Kim HS, Choi EC, Delgado M, Granja JR, Khasanov A, Kraehenbuehl K, Long G, Weinberger DA, Wilcoxen KM, Ghadiri MR. Antibacterial agents based on the cyclic D,L-α-peptide architecture. *Nature.* 2001; **412**: 452–455.
10 Ogura KJ. Molecular recognition by crystalline dipeptides. *Japan Oil Chem. Soc.* 1994; **43**: 779–786.
11 Akazome M, Hirabayashi A, Takaoka K, Nomura S, Ogura K. Molecular recognition of L-leucyl-L-alanine: enantioselective inclusion of alkyl methyl sulfoxides. *Tetrahedron* 2005; **61**: 1107–1113.
12 Kaufman DB, Hayes T, Buettner J, Hammond DJ, Carbonell RG. Chromatographic resolution of tryptophan enantiomers with L-Leu-L-Leu–L-Leu peptide. Effects of mobile phase composition and chromatographic support. *J. Chromatogr. A* 2000; **874**: 21–26.
13 Görbitz CH, Rise F. Template-directed supramolecular assembly of a new type of nanoporous peptide-based material. *J. Pept. Sci.* 2008; **14**: 210–216.
14 Gao X, Matsui H. Peptide-based nanotubes and their applications in bionanotechnology. *Adv. Mater.* 2005; **17**: 2037–2050.
15 Yan X, Cui Y, He Q, Wang K, Li J, Mu W, Wang B, Ou-yang Z. Reversible transitions between peptide nanotubes and vesicle-like structures including theoretical modeling studies. *Chem. Eur. J.* 2008; **14**: 5974–5980.
16 Rica R, Matsui H. Applications of peptide and protein-based materials in bionanotechnology. *Chem. Soc. Rev.* 2010; **39**: 3499–3509.
17 Kasai S, Ohga Y, Mochizuki M, Nishi N, Kadoya Y, Nomizu M. Multifunctional peptide fibrils for biomedical materials. *Biopolymers (Peptide Science)*. 2004; **76**: 27–33.
18 Yang Y, Khoe U, Wang X, Horii A, Yokoi H, Zhang S. Designer self-assembling peptide nanomaterials. *Nano Today.* 2009; **4**: 193–210.
19 Gazit E. Self-assembled peptide nanostructures: the design of molecular building blocks and their technological utilization. *Chem. Soc. Rev.* 2007; **36**: 1263–1269.
20 Rosenman G, Beker P, Koren I, Yevnin M, Bank-Srour B, Mishina E, Semin S. Bioinspired peptide nanotubes: deposition technology, basic physics and nanotechnology applications. *J. Pept. Sci.* 2011; **17**: 75–87.
21 Kol N, Adler-Abramovich L, Barlam D, Shneck RZ, Gazit E, Rousso I. Self-assembled peptide nanotubes are uniquely rigid bioinspired supramolecular structures. *Nano Lett.* 2005; **5**: 1343–1346.
22 Yan X, Zhu P, Li J. Self-assembly and application of diphenylalanine-based nanostructures. *Chem. Soc. Rev.* 2010; **39**: 1877–1890.
23 Burchell TJ, Soldatov DV, Ripmeester JA. Crystal structure of the co-crystal ALA-VAL·ALA·H_2O: a layered inclusion compound. *J. Struct. Chem.* 2008; **49**: 188–191.
24 Burchell TJ, Soldatov DV, Enrighta GD, Ripmeester JA. The ability of lower peptides to form co-crystals: inclusion compounds of Leu-Leu-Leu tripeptide with pyridine and picolines. *Cryst. Eng. Comm.* 2007; **9**: 922–929.
25 Soldatov DV, Moudrakovski IL, Ripmeester JA. Dipeptides as Microporous Materials. *Angew. Chem. Int. Ed.* 2004; **43**: 6308–6311.
26 Gorbatchuk VV, Ziganshin MA, Solomonov BN, Borisover MD. Vapor sorption of organic compounds on human serum albumin. *J. Phys. Org. Chem.* 1997; **10**: 901–907.
27 Mironov NA, Breus VV, Gorbatchuk VV, Solomonov BN, Haertle T. Effects of hydration, lipids, and temperature on the binding of the

volatile aroma terpenes by a-lactoglobulin powders. *J. Agric. Food Chem.* 2003; **51**: 2665–2673.
28 Hamley IW. Nanotechnology with soft materials. *Angew. Chem. Int. Ed.* 2003; **42**: 1692–1712.
29 Moudrakovski IL, Soldatov DV, Ripmeester JA, Sears DN, Jameson CJ. Xe NMR line shapes in channels of peptide molecular crystals. *PNAS.* 2004; **101**: 17924–17929.
30 Ryu J, Park CB. High-temperature self-assembly of peptides into vertically well-aligned nanowires by aniline vapor. *Adv. Mater.* 2008; **20**: 3754–3758.
31 Ryu J, Park CB. High stability of self-assembled peptide nanowires against thermal, chemical, and proteolytic attacks. *Biotechnol. Bioeng.* 2010; **105**: 221–230.
32 Ryu J, Park CB. Solid-phase growth of nanostructures from amorphous peptide thin film: effect of water activity and temperature. *Chem. Mater.* 2008; **20**: 4284–4290.
33 Efimova IG, Ziganshin MA, Gorbatchuk VV, Soldatov DV, Ziganshina SA, Chuklanov AP, Bukharaev AA. Formation of nanoislands on the surface of thin dipeptide films under the effect of vaporous organic compounds. *Protect. Metals Phys. Chem. Surf.* 2009; **45**: 525–528.
34 Gorbatchuk VV, Ziganshin MA, Solomonov BN. Supramolecular interactions of solid human serum albumin with binary mixtures of solvent vapors. *Biophys. Chem.* 1999; **81**: 107–123.
35 Armarego WLF, Perrin DD. *Purification of Laboratory Chemicals*, Butterworth, Oxford, 2000.
36 Yakimova LS, Ziganshin MA, Sidorov VA, Kovalev VV, Shokova EA, Tafeenko VA, Gorbatchuk VV. Molecular recognition of organic vapors by adamantylcalix[4]arene in QCM sensor using partial binding reversibility. *J. Phys. Chem. B* 2008; **112**: 15569–15575.
37 Safina GD, Validova LR, Ziganshin MA, Stoikov II, Antipin IS, Gorbatchuk VV Using clathrate pseudopolymorphism for a single sensor detection of target component in the headspace of liquid mixture. *Sensors and Actuators B.* 2010; **148**: 264–268.
38 Gorbatchuk VV, Tsifarkin AG, Antipin IS, Solomonov BN, Konovalov AI, Lhotak P, Stibor I. Nonlinear structure-affinity relationships for vapor guest inclusion by solid calixarenes. *J. Phys. Chem. B* 2002; **106**: 5845–5851.
39 Solomonov BN, Konovalov AI. Thermochemistry of the solvation of organic non-electrolytes. *Russ. Chem. Rev.* 1991; **60**: 45–68.
40 Gorbatchuk VV, Ziganshin MA, Mironov NA, Solomonov BN. Homotropic cooperative binding of organic solvent vapors by solid trypsin. *Biochim. Biophys. Acta* 2001; **1545**: 326–338.
41 Gorbatchuk VV, Mironov NA, Solomonov BN, Habicher WD. Biomimetic cooperative interactions of dried cross-linked poly(*N*-6-aminohexylacrylamide) with binary mixtures of solvent vapors. *Biomacromolecules* 2004; **5**: 1615–1623.
42 Gerasimov AV, Ziganshin MA, Vandyukov AE, Kovalenko VI, Gorbatchuk VV, Caminade A-M, Majoral J-P. Specific vapor sorption properties of phosphorus-containing dendrimers. *J. Colloid Interface Sci.* 2011; **360**: 204–210.

